Case Study: Numerical Investigation of Lateral Stability of Non-prismatic Double Web-tapered Prestressed Reinforced Concrete Girder

Wael Hameedi[1*], István Völgyi[1]

[1] Department of Structural Engineering, Faculty of Civil Engineering, Budapest University of Technology and Economics, Műegyetem rkp. 3, H-1111 Budapest, Hungary
[*] Corresponding author, e-mail: wael.hameedi@edu.bme.hu

Abstract

This study presents a comprehensive numerical investigation into the lateral stability of non-prismatic, double web-tapered prestressed reinforced concrete girders using advanced finite element modeling (FEM) in ATENA-GiD, validated against experimental results. The analysis examines the influence of key parameters, including initial lateral imperfections (ILI), rubber bearing pad stiffness, concrete tensile strength, load application method, and the effectiveness of fork support restraints. Results reveal that increasing ILI amplifies mid-span lateral displacement by up to 55%, compromising stability. Conversely, stiffer rubber pads improve restraint performance, reducing lateral displacement by 42%, while higher concrete tensile strength decreases lateral displacement by 32% and delays crack formation. Additional parametric studies highlight that the application of eccentric loads, common in experimental and real-world setups, induces secondary torsional effects that reduce lateral stability. A centric load application condition improved performance by reducing lateral displacement by 14%. Moreover, incorporating fully hardened fork supports at girder ends led to a 60% reduction in out-of-plane displacement, demonstrating their essential role in suppressing lateral-torsional buckling. These findings underscore the critical importance of accounting for geometric imperfections, support detailing, load positioning, and material properties in the design of slender, long-span, non-prismatic girders to ensure optimal stability and structural safety.

Keywords

non-prismatic, double web-tapered, lateral stability, prestressed concrete, finite element analysis

1 Introduction

A beam with varying cross-sectional properties is termed a non-prismatic beam. This type of beam may feature tapered, arched, or other diverse shapes to optimize structural performance and aesthetics [1]. Reinforced concrete structures are well-known for their substantial self-weights, which present greater challenges over extended spans. However, utilizing non-prismatic sections can significantly reduce the self-weight of RC constructions. This approach not only alleviates weight-related issues but also offers the potential for aesthetically appealing architectural designs [2–4]. While prismatic members are most commonly employed in engineering construction, economic and architectural considerations often require the use of irregularly shaped members designed to support specific applied loads [5]. In designing tall structures, reducing roof heights through the use of variable cross-section beams is a beneficial approach. Variable sections are now widely incorporated across nearly all structural types [6–8]. These beams function as structural elements designed to withstand bending, shear, and torsion forces. Additionally, they can accommodate various service utilities through integrated openings [8, 9]. This approach provides options to reduce ceiling heights tailored to specific building requirements, effectively lowering construction costs and material usage. Additionally, variable cross-section beams can be utilized in the foundations of residential developments or complexes, particularly where integration with existing and new service connections poses challenges [10]. Hollow sections or openings within beams provide secure routes for electrical, plumbing, or transmission installations, while also decreasing the structure's total weight [11, 12]. However, dealing with long-span non-prismatic beams, particularly those with a high slenderness ratio at their critical cross-sections, raises

significant concerns regarding their lateral stability (LS). In contrast, for prismatic beams such as those with rectangular cross-sections, numerous studies in the literature have focused on lateral torsional buckling (LTB) [13–18]. Sherbourne and Pandey [19] proposed a more accurate analytical model for determining the lateral-torsional stability of beams subjected to unequal end moments. Their approach introduces a refined moment modification factor (ω) that accounts explicitly for beam slenderness, moment gradient, and end restraint conditions factors often oversimplified in earlier formulations. By superimposing torsional and warping buckling modes, they derived a closed-form parametric expression for ω, which yields improved estimates of the critical buckling moment, particularly for simply supported beams. Their model was supported by classical, Galerkin, and finite element solutions, demonstrating greater accuracy and reduced conservatism compared to existing methods. Adding to that, in a two-part study, Mast [20, 21] extensively investigated the lateral stability of prismatic long prestressed I-section concrete beams under different support conditions. Part 1 (1989) [20] focused on beams suspended from lifting loops, introducing a simplified method to evaluate lateral bending stability based on roll axis geometry, initial imperfections, and tilt angle limits. Mast [20] derived analytical expressions for the factor of safety, showing how small shifts in lifting point location can significantly improve stability. He also highlighted the limitations of traditional buckling formulas, advocating for a more equilibrium-based approach tailored to the high torsional stiffness of concrete beams. Part 2 (1993) [21] expanded the analysis to beams supported from below, such as during transportation on trucks or resting on elastomeric pads. This part addressed the nonlinear behavior of supports and post-cracking response of the beam, verified through full-scale testing. Mast [21] introduced the concept of radius of stability and proposed new equations that incorporate rotational spring stiffness and cracked section behavior, providing a more comprehensive stability assessment for practical applications. Mottram [22] conducted a detailed investigation into the lateral instability of slender precast concrete beams during lifting operations. Their work emphasized the critical role of lifting point placement, initial sweep imperfections, and the beam's flexural stiffness about its weak axis. Using both theoretical formulations and experimental data, they derived equations to assess the lateral displacements and tilt angles that develop during lifting. The study also introduced a simple design method to determine safe lifting

configurations, validated by physical tests on full-scale beams. Their findings provided practical design curves and highlighted how even minor changes in lifting setup or geometric imperfections can significantly affect stability. Later on, Helwig et al. [23] examined the lateral instability of precast prestressed concrete beams during lifting using a combination of theoretical modeling and experimental validation. Their study focused on beams with varying cross-sections and lifting point locations, emphasizing how geometric imperfections and weak-axis flexural stiffness influence stability. The authors developed analytical expressions for estimating critical tilt angles and lateral displacements, and validated them with physical tests on full-scale beams. Their work showed that traditional design approaches often underestimate the effects of initial imperfections, leading to unsafe predictions. The study concluded with practical guidelines for safer lifting configurations in precast operations. Also, Stratford and Burgoyne [24] developed a comprehensive nonlinear finite element model to investigate the lateral stability of precast concrete beams with various cross-sections during handling and transportation. Their study accounted for geometric imperfections, cracking behavior, and the influence of support conditions, including lifting point placement and suspension methods. They validated their model using experimental results, demonstrating good agreement and highlighting the importance of capturing nonlinear behavior in stability predictions. The study emphasized that traditional linear elastic methods tend to underestimate the risk of lateral instability, particularly in long-span beams. Their findings offer practical guidance for safer lifting configurations and support designs in precast beam handling. Additionally, Revathi and Menon [25] investigated the critical buckling moments in slender RC beams with rectangular cross sections, they highlighted that current design codes may not effectively prevent lateral instability. Experimental results indicate that even within code limits, slender beams can buckle. The authors proposed an improved analytical model for predicting critical buckling moments, aligning better with experimental outcomes, especially for under-reinforced sections. The study calls for refining design standards to enhance stability provisions. Additionally, Lee and Kalkan [26] developed an analytical equation to estimate the critical buckling load for RC beams with initial geometrical imperfections for rectangular cross sections. Yücesoy and Coşkun [27] presented a numerical investigation into the lateral stability of precast concrete beams during lifting,

focusing on the impact of lifting point location, beam geometry, and material properties. Using a detailed finite element model, the study examined the development of lateral displacements and rotations under self-weight, with and without initial imperfections. Their results highlighted the sensitivity of beam stability to lifting configurations, especially in long-span members. The authors also proposed critical guidelines for optimal lifting point locations to reduce instability risks. The findings contribute valuable insight into safe lifting practices and improve the reliability of handling operations for precast elements. All previously mentioned studies focused on prismatic beams with simple geometric properties, and none explored the LS of non-prismatic beams, particularly those with varying cross-sectional shapes. This study adopts a non-prismatic double web-tapered RC beam with an I-section as the case study. The cross-sectional depth varies along the span, reaching its maximum at the mid-span and its minimum at the ends, resulting in variable stiffness along the span. Such complex geometry makes it challenging to calculate the critical buckling load directly using equations. Therefore, the finite element method (FEM) is employed as an efficient approach to investigate the stability behavior of these types of beams. An advanced FEM model was developed and validated against experimental behavior. This experimental test was conducted in our previous study [28] to explore the LS of a longitudinally assembled girder made of precast reinforced and prestressed concrete parts.

2 Experimental program overview

The experimental study was originally focused on the buckling moment capacity of a longitudinally assembled girder of precast RC members that consist of a long central part and two small parts at the ends, using commercial bolted connections products that are developed for assembling precast buildings. The reason for the assembly is to have longer span girders, especially with a central prestressed RC member. Utilizing such a method will lead to more reliable and economical products. For example,

the need for an extended prestress bench is not required, and it is easier to handle and transport, etc. It follows logically that any unfavorable movements at the connection zones due to the separations between the bolted connections caused by misalignment of the connection components will lead to a substantial increase in second-order effects. The loading was executed using concrete blocks, each weighing 1575 kg (16 kN); the process consisted of 18 steps, with a pair of concrete blocks placed in each step, except for steps 9 and 18, where only one block is added. The first pair is positioned 3.3 m from the support to mitigate shear cracks at the girder's notches. A 20 cm tolerance is maintained between loading pairs for crane movement. The process begins at the right-end support, progressing toward mid-span, placing 17 blocks. It is then repeated in reverse from the left-end support to mid-span, adding another 17 blocks as illustrated in Fig. 1. There were three tests, AG1-A and AG1-B, executed on specimen AG1, while a test labeled AG2 was executed on the second specimen AG2. In the experiment, the adopted preloads at all tests were high enough to make a perfect connection, although the second specimen lost its stability and failed due to a combined failure of rollover and lateral torsional buckling, due to insufficient lateral supports at the ends, as well as large initial imperfections of the prestressed member. The experimental findings revealed that the separation in the connection zones was less than 0.6 mm, attributed to the high preload. Consequently, this separation had a negligible effect on the LS of the assembled girder. Therefore, to simplify the FEM model, the whole girder with the same dimensions as the experimental girder was modeled without considering the bolted connections between individual parts.

3 Finite element analysis in ATENA-GiD

ATENA-GiD software [29] was employed to conduct numerical analysis. Where ATENA (v5.9.2) is a widely used finite element-based software typically used for nonlinear analysis of reinforced concrete (see, for example, studies [30, 31]), while GiD (v16.0.6) is a versatile and
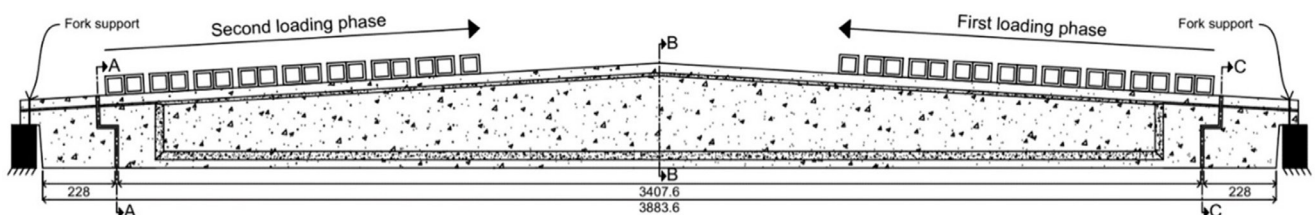

Fig. 1 Experimental setup (dimensions in mm) [28]

user-friendly software application that features an interactive graphical user interface designed to prepare input data for ATENA analysis. It is primarily used for geometric modeling, allowing users to define, prepare, and visualize all the data associated with numerical simulations. With its intuitive interface and robust capabilities, GiD simplifies the process of setting up and managing complex simulation models, making it an essential tool for numerical analysis.

In the present numerical study, the numerical analysis used for simulating the LS of the specimen AG2 from the experimental study. Furthermore, the girder was modeled as one piece without considering a three-pieces structure because the maximum separation value at all the connection zones was less than 0.6 mm, indicating a perfect connection condition, and this is because of relatively high applied preload at all connection's nuts (about 1.2 kNm). Fig. 2 shows the stress-strain relationship of the concrete and reinforcement rebars as well as prestressing tendons. Fig. 3 illustrates the finite element mesh and boundary conditions for the girder. Three types of elements were used:

1. the linear hexahedral element type assigned to all concrete beam volumes;
2. linear tetrahedral element type assigned for the steel plates; and
3. linear truss element type assigned for the reinforcing bars.

Additionally, a mesh-independence study was performed by refining the finite-element mesh until changes in the monitored responses (e.g., load-displacement behavior) between successive meshes fell within the chosen tolerance. The final mesh was selected as the coarsest mesh satisfying this criterion, thereby reducing computational time while maintaining result accuracy. All the concrete volumes are meshed structurally, with a size of 200 mm assigned to all lines of concrete volumes. In GiD, reinforcement bars can be modelled using 1D elements with perfect or predefined bond law between reinforcements and concrete, or by using 3D elements for more sophisticated bond representation [32]. In this study 1D reinforcement bars elements were used with perfect bond. Since the loading process in the experimental test was done by utilizing concrete blocks, where the C.G. of these blocks is clearly located above the upper surface of the girder, and due to the girder initial lateral imperfection (ILI), there will be a small lever arms between the roll-axis of the girder and the C.G. of the blocks, and that will create torsional moments, so to include this effect in the modeling, the loading steel plate was modeled with a cylindrical rod, with a height equal to half the block's height, on top of it, and the block weight is represented by a point load that is applied at the top of that rod. Additionally, for numerical purposes, external steel plates, referred to as prestressing plates, were fixed at each side of the prestressing area to avoid concrete damage due to high prestressing forces. Three monitoring points were considered at the mid-span of the girder to record the displacements: the first one is placed on the upper flange's edge at the outer face of the girder to capture the lateral displacement; the second is positioned at the lower flange's edge at the inner face of the girder to capture the vertical displacement of the girder; and the third monitoring point is placed at the center of gravity of the girder at the mid-span in order to record the ILI after the application of the prestressing force. Regarding the boundary conditions in the model,
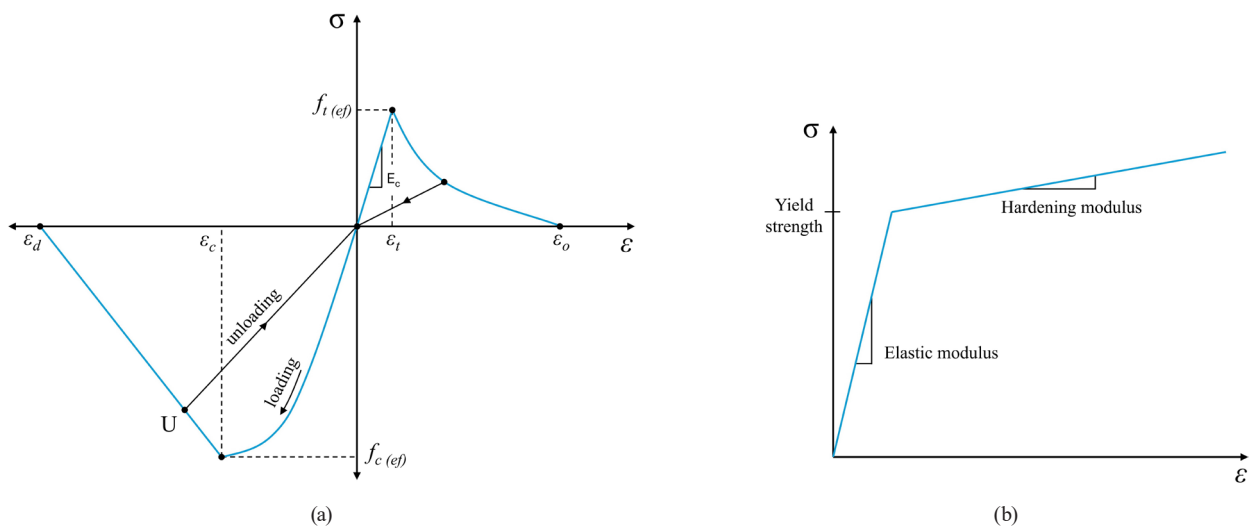

Fig. 2 Stress-strain relationship of (a) concrete (b) reinforcement rebars and prestressing strands
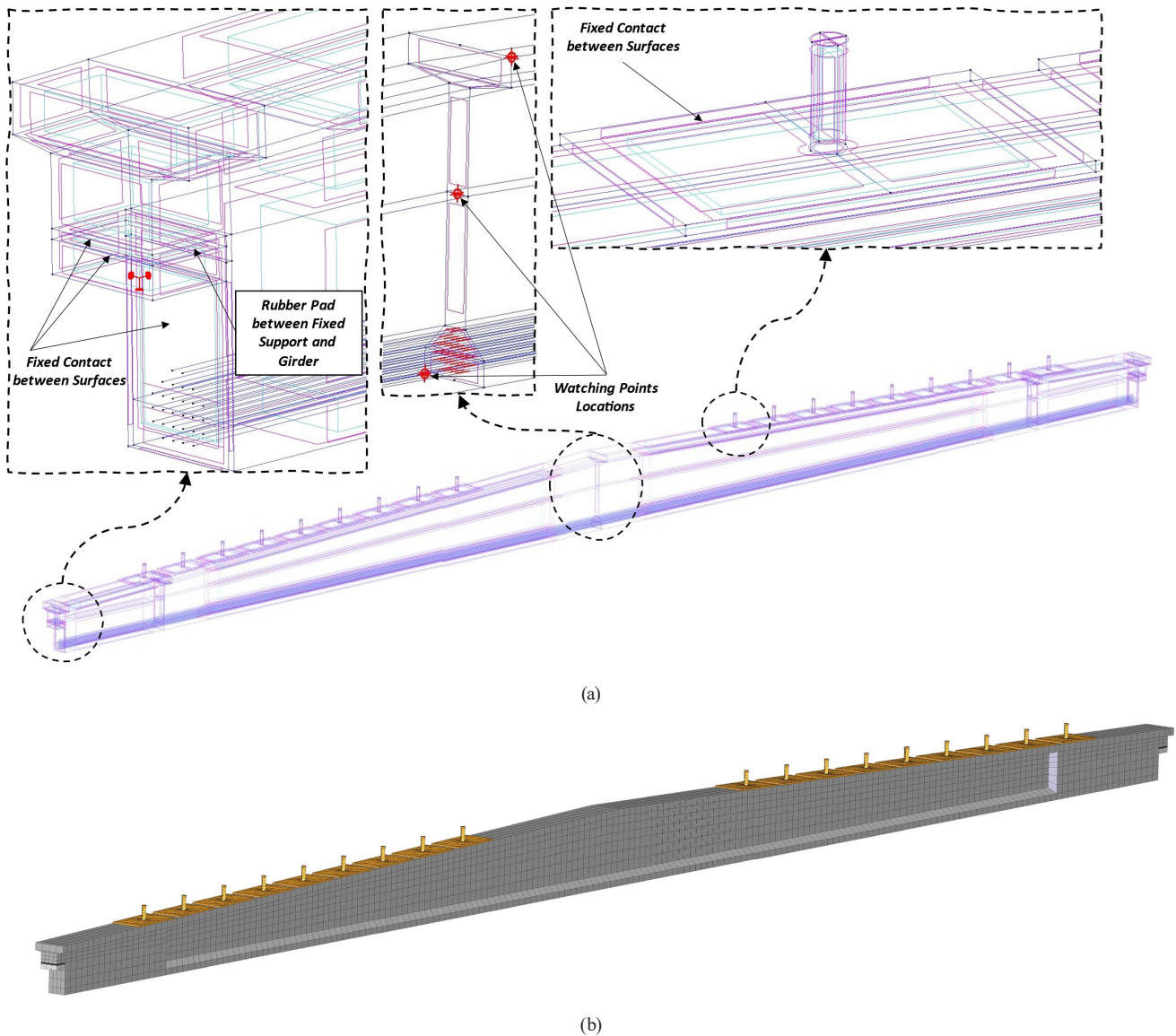
(a)

(b)

Fig. 3 (a) Boundary conditions (b) Meshing for finite element model

a "fixed contact for surface" condition was utilized in the following cases: between the loading steel plates and the upper surface of the girder, between the prestressing steel plates and the side faces of the girder, between the girder and rubber bearing pads, and between the rubber pad and the rigid concrete support. "Constraint for surface" conditions were that translations in (X, Y, Z) directions were forbidden and were assigned to the bottom surface of the rigid concrete support to simulate the experimental test support configuration. In addition, fork supports applied in the real test were also modeled as two 25-mm vertical reinforcing bars at both supports to enhance the lateral rigidity of the girder. The properties of concrete are generated by EuroCode2 for the characteristic safety format for C50/60 concrete type. All material properties used on the

Table 1 Material properties used in FEM software

| Material	Property	Quantity	Unit
Concrete (characteristic values)	Young's Modulus - E_{cm}	37000	MPa
	Poisson's Ratio - v_c	0.2	----
	Tension Strength - f_{ctk}	2.9	MPa
	Compression Strength - f_{ck}	−50	MPa
	Tension Stiffening	0.36	----
Steel plates	Young's Modulus - E_{sp}	200	GPa
	Poisson's Ratio - v_{sp}	0.3	----
Rubber bearing pad	Young's Modulus - E_r	79	MPa
	Poisson's Ratio - v_r	0.4	----
Normal reinforcement bars	Young's Modulus - E_s	200	GPa
	Yield strength - f_{yk}	500	MPa
Prestressing strands	Young's Modulus - E_p	200	GPa
	Tensile strength - f_{pk}	1860	MPa

FEM software can be found in Table 1.

3.1 Validation of the FEM model

The initial geometric imperfection of a girder was introduced into the finite element modeling by utilizing the eccentricity of the prestressing forces. To achieve this effect, it is essential to maintain an appropriate difference in prestressing forces between the left and right groups of the prestressing tendons. A good agreement achieved between FE analysis and AG2 experimental test for both; vertical displacement vs load and lateral displacement vs load as illustrated in Fig. 4.
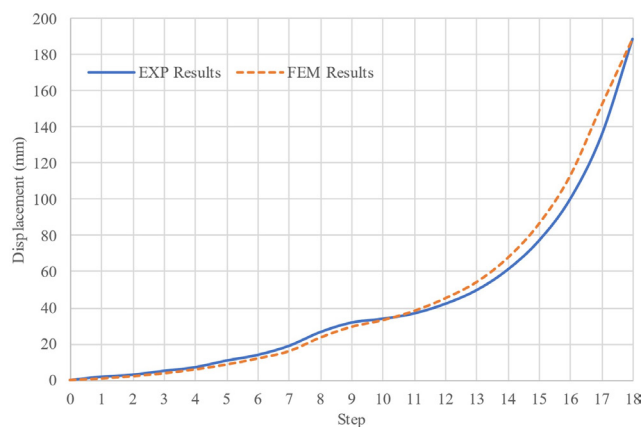
4 Parametric study

A parametric study is performed employing the validated FE model to further investigate the LS of the girder loaded with concrete blocks. Three parameters are selected for parametric study, namely, ILI, modulus of elasticity of the rubber bearing pad, and the tensile strength of concrete.

4.1 Effect of initial lateral imperfection
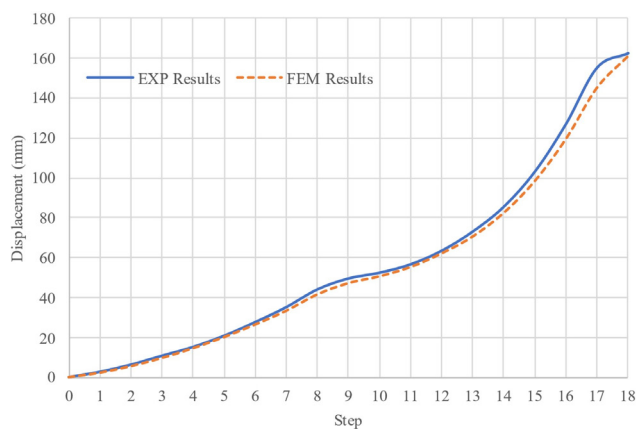
(a)

(b)

Fig. 4 Comparison of experimental and FEM results for AG2
(a) vertical displacement (b) lateral displacement

A total of four models with 69.81 mm, 56.21 mm, 35.38 mm, 24.77 mm ILIs were analyzed in ATENA-GiD and their lateral displacements were compared with those of validated model as shown in Fig. 5. It is worth mentioning that the measured ILI of the specimen AG2 from the experiment equals to 46 mm [28]. The L.I. values that vary from one another can be generated by applying different eccentric prestressing forces. It can be concluded that if the ILI is increased, then the lateral displacement will also increase with the same loads, and consequently, the lateral bending capacity of the model will decrease.

4.2 Effect of rubber bearing pad stiffness

The LS of four FEM models supported by rubber pads with varied elastic modulus was analyzed using ATENA-GiD. By employing rubber pads with lower stiffness, the beam LS drops in simulation results. The lateral displacements for all models are shown in Fig. 6. However, in the case of the utilization of rubber pad with an elastic modulus of 60 MPa, the model becomes laterally unstable prior to reaching the full loading, and it will experience increasing lateral displacement and ultimately result in LTB failure of the girder, as indicated by the steep increase in the yellow curve in Fig. 6. Employing stiffer rubber pads will
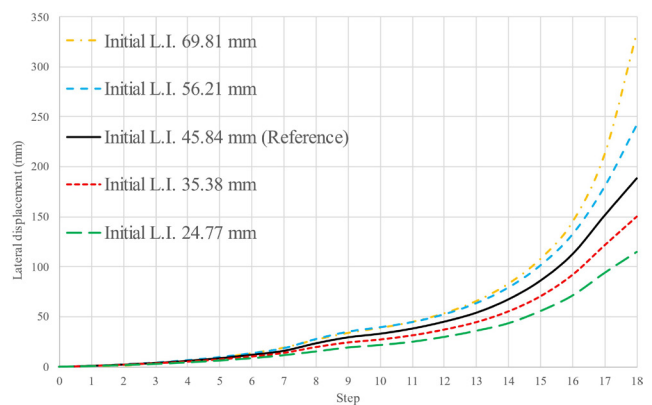

Fig. 5 Effect of initial lateral imperfection on LS of the girder
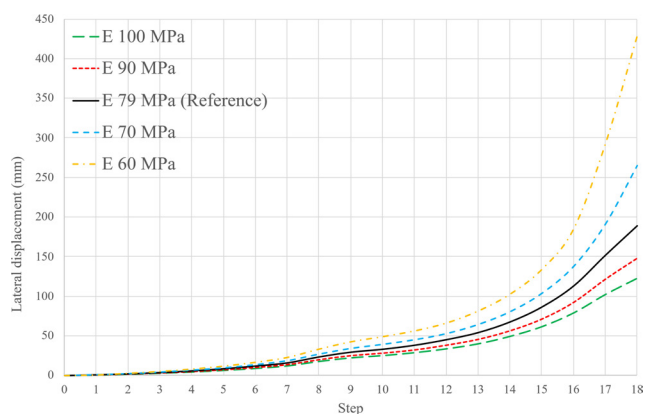

Fig. 6 Effect of rubber pad elastic modulus on LS of the girder

provide higher LS, especially for a short period of temporary girder support before integration into a structure. This suggests that the rubber property selection needs to be targeted at structural configurations to avoid failure modes, such as lateral torsional buckling.

4.3 Effect of concrete's tensile strength

The tensile strength of concrete significantly impacts the onset of the cracks caused by the applied loads. Since concrete cracking directly affects lateral bending and torsional rigidities, especially in long, slender beams, it is important to consider the concrete tensile strength in parametric studies. Four models with different f_{ctk} values are analyzed, where f_{ctk} is the characteristic tensile strength of concrete material, which is equal to the formula for 5% fractile tensile strength (f_{ctk}, 0.05), i.e., 0.7 of the mean value of axial tensile strength of concrete (f_{ctm}).

Modifications to the concrete characteristic compressive strength were also made according to the EC2 equation, as shown in Eq. (1).

$$f_{ctm} = 0.3 \times f_{ck}^{(2/3)} \leq C50/60 \qquad (1)$$

Fig. 7 shows the lateral displacement for the analyzed and validated models. Using higher tensile strength concrete will increase the lateral bending and torsional rigidities, hence increasing LS, and vice versa. The model with a tensile strength of 2.3 MPa lost its LS after step 16, which can be seen clearly in Fig. 7, where the deflection increased dramatically.

4.4 Effect of load application method on lateral stability

In the original experiment, loading was applied using concrete blocks, which were modeled as point loads applied on top of vertical steel rods welded to the loading steel plat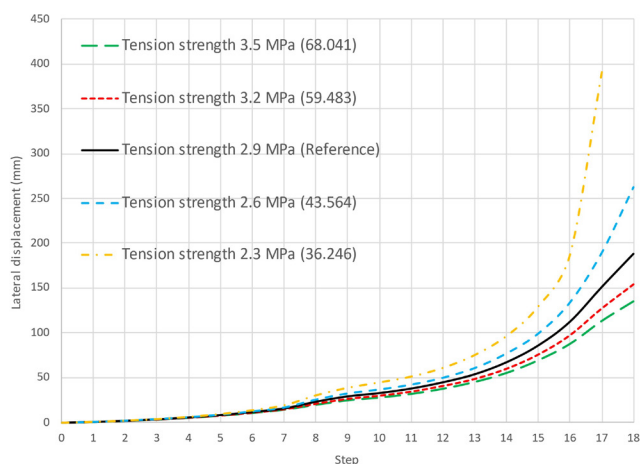es. This arrangement effectively raised the point of load application above the girder's centroidal axis, introducing a vertical eccentricity relative to the neutral axis of the structure. Due to the initial geometrical imperfections present in the girder, such as deviations in alignment caused by fabrication tolerances or prestressing-induced curvature, this elevation created a lever arm between the center of gravity of the applied loads and the roll-axis of the girder. As a result, torsional moments were unintentionally introduced during loading, which magnified the lateral displacements through second-order effects and compromised the girder's lateral stability. To assess the influence of this elevated loading, a comparative parametric study was conducted by modifying the load application method: instead of applying point loads through the top of the steel rods, the loads were directly applied to the upper surface of the loading steel plates in the finite element model, thereby achieving a centric loading condition. This change effectively removed the vertical offset and aligned the loads with the centroidal axis of the girder, eliminating the torsional moment generated by eccentricity. The results of the finite element analysis clearly demonstrate the structural advantage of centric loading. As evident from the load–displacement curves as showed in Fig. 8, the maximum lateral deflection at midspan decreased from 188.5 mm (in the eccentric case) to 162.0 mm (in the centric case), indicating a notable 14% reduction in lateral displacement. This improvement in lateral stability confirms that eccentric loading, when combined with initial imperfections, significantly contributes to instability. Therefore, careful attention to the position of load application particularly in precast or temporary support scenarios can greatly enhance the safety and performance of slender, non-prismatic prestressed girders. This parametric finding underscores the importance of eliminating secondary torsional effects by maintaining centric load conditions wherever feasible during both testing and real-world construction.
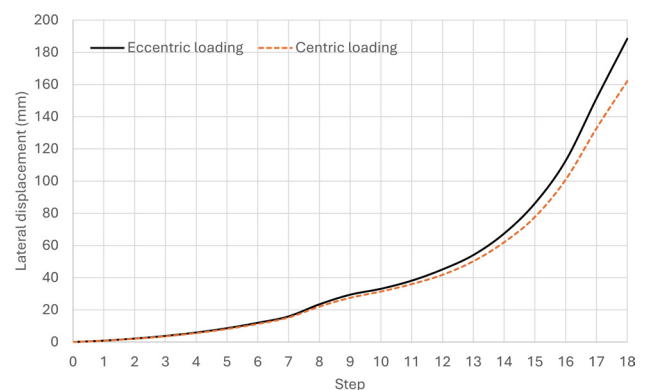

Fig. 7 Effect of concrete's tensile strength on LS of the girder

Fig. 8 Effect of load application method on lateral stability

4.5 Enhancement of lateral stability using fork supports

The effectiveness of fork supports in enhancing the lateral stability of the girder was evaluated through both experimental observation and finite element modeling. In the experimental setup, two vertical steel bars (⌀25 mm) were embedded at each support and grouted to serve as lateral restraints. However, due to insufficient curing time of the grout, the bond between the steel and surrounding concrete was inadequate. This compromised the restraint action, allowing significant lateral movement under loading.

To assess the ideal performance of fork supports, a refined finite element model was developed with fully effective fork restraints rigidly embedded in properly hardened concrete. The resulting lateral displacement response, plotted against load steps, is presented in Fig. 9. The experimental results (EXP Results) exhibit a sharp increase in lateral deflection beyond step 14, indicating the onset of instability. In contrast, the FE model with fully functional forks shows a stable and controlled lateral response throughout loading, with no signs of buckling. This comparison demonstrates that properly executed fork supports can reduce lateral deflection by over 60% and effectively prevent lateral-torsional instability. The numerical model confirms that stiff, well-anchored fork supports at the girder ends are critical in suppressing second-order effects and maintaining structural integrity, especially in slender, non-prismatic configurations. These findings highlight the importance of properly installing and curing support details in precast girder systems.

5 Conclusions

This paper presents a numerical analysis of LS of a non-prismatic double web-tapered prestressed reinforced concrete
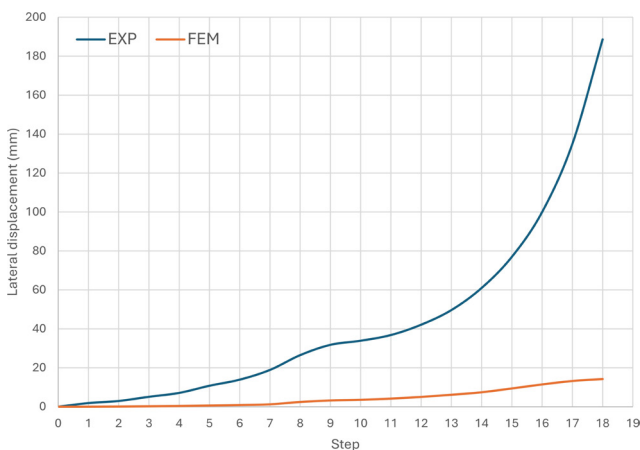

Fig. 9 Fork support constraints existence

beam. A good agreement between previous experimental and current numerical results was achieved. An intensive parametric study was carried out to investigate the effect of ILI, Young's modulus of the rubber bearing pad where the girder is sitting, and the tensile strength of the concrete on the LS of the tested as well as the effect of different load application methods and the inclusion of the fork supports as a lateral constraint, and the following conclusions were drawn:

1. ILI has a significant effect on the LS of the assembled girder by increasing the ILI (from 45.84 mm to 69.81 mm) the midspan horizontal deflection will increase by 55.48%; conversely, when decreasing the ILI (from 45.84 mm to 24.77 mm), the midspan horizontal deflection will decrease by 48.3%.

2. The modulus of elasticity of the rubber bearing pad where A.G. is sitting has a critical role in the LS of the beam. Decreasing the modulus of elasticity of the rubber from 79 MPa to 60 MPa will result in a loss of stability due to increased out-of-plane displacement. Meanwhile, increasing the rubber elasticity from 79 MPa to 100 MPa will decrease the midspan lateral displacement by 42.23%.

3. Concrete tensile strength property has a direct effect on the LS of the girder because it controls the cracking formation initiation; using a lower value of f_{ctk} (from 2.9 MPa to 2.3 MPa) will make the girder lose its LS after step 16 (after placing loading blocks 30th and 31st) and combined failure takes place then. Meanwhile, concrete with higher tensile strengths (from 2.9 MPa to 3.5 MPa) will decrease the midspan lateral deflection by 32.59%.

4. Applying the load centrically reduced the maximum lateral deflection by 14% (from 188.5 mm to 162.0 mm), confirming that eliminating vertical eccentricity significantly improves the lateral stability of slender, non-prismatic girders.

5. The inclusion of properly installed and fully hardened fork supports reduced lateral deflection by over 60%, clearly demonstrating their critical role in enhancing the lateral stability and preventing torsional failure in slender, non-prismatic girders.

More studies are needed to consider further factors that may affect the LS of a non-prismatic double web-tapered prestressed reinforced concrete beam, and those factors are the initial rotational angle of the main beam's section at the mid-span, rotation of the supports.

References

[1] Al-Ahmed, A. H. A., Al-Zuhairi, A. H., Hasan, A. M. "Behavior of reinforced concrete tapered beams", Structures, 37, pp. 1098–1118, 2022.
https://doi.org/10.1016/j.istruc.2022.01.080

[2] Alshimmeri, A. J. H., Jaafar, E. K., Shihab, L. A., Al-Maliki, H. N. G., Al-Balhawi, A., Zhang, B. "Structural Efficiency of Non-Prismatic Hollow Reinforced Concrete Beams Retrofitted with CFRP Sheets", Buildings, 12(2), 109, 2022.
https://doi.org/10.3390/buildings12020109

[3] Attarnejad, R., Shahba, A. "Application of differential transform method in free vibration analysis of rotating non-prismatic beams", World Applied Sciences Journal, 5(4), pp. 441–448, 2008.

[4] Han, L.-H., Li, W., Bjorhovde, R. "Developments and advanced applications of concrete-filled steel tubular (CFST) structures: Members", Journal of Constructional Steel Research, 100, pp. 211–228, 2014.
https://doi.org/10.1016/j.jcsr.2014.04.016

[5] Rogers, B. G., Munse, W. H., Jr. "Plastic Analysis and Design of Non-Prismatic Members", Journal of the Structural Division, 91(5), pp. 299–324, 1965.
https://doi.org/10.1061/JSDEAG.0001334

[6] Alnauimi, A. S., Bhatt, P. "Direct design of hollow reinforced concrete beams. Part II: experimental investigation", Structural Concrete, 5(4), pp. 147–160, 2004.
https://doi.org/10.1680/stco.2004.5.4.147

[7] Alnuaimi, A. S., Al-Jabri, K. S., Hago, A. "Comparison between solid and hollow reinforced concrete beams", Materials and Structures, 41(2), pp. 269–286, 2008.
https://doi.org/10.1617/s11527-007-9237-x

[8] Balaji, G., Vetturayasudharsanan, R. "Experimental investigation on flexural behaviour of RC hollow beams", Materials Today: Proceedings, 21, pp. 351–356, 2020.
https://doi.org/10.1016/j.matpr.2019.05.461

[9] Hassan, N. Z., Ismael, H. M., Salman, A. M. "Study behavior of hollow reinforced concrete beams", International Journal of Current Engineering and Technology, 8(6), pp. 1640–1651, 2018.
https://doi.org/10.14741/ijcet/v.8.6.19

[10] Hemzah, S. A., Alyhya, W. S., Hassan, S. A. "Experimental investigation for structural behaviour of self-compacting reinforced concrete hollow beams with in-place circular openings strengthened with CFRP laminates", Structures, 24, pp. 99–106, 2020.
https://doi.org/10.1016/j.istruc.2020.01.008

[11] Abbass, A., Abid, S., Özakça, M. "Experimental Investigation on the Effect of Steel Fibers on the Flexural Behavior and Ductility of High-Strength Concrete Hollow Beams", Advances in Civil Engineering, 2019(1), 8390345, 2019.
https://doi.org/10.1155/2019/8390345

[12] Zhou, M., Shang, X., Hassanein, M. F., Zhou, L. "The differences in the mechanical performance of prismatic and non-prismatic beams with corrugated steel webs: A comparative research", Thin-Walled Structures, 141, pp. 402–410, 2019.
https://doi.org/10.1016/j.tws.2019.04.049

[13] Hansell, W., Winter, G. "Lateral Stablity of Reinforced Concrete Beams", ACI Journal Proceedings, 56(9), pp. 193–214, 1959.
https://doi.org/10.14359/8091

[14] Sant, J. K., Bletzacker, R. W. "Experimental Study of Lateral Stability of Reinforced Concrete Beams", ACI Journal Proceedings, 58(12), pp. 713–736, 1961.
https://doi.org/10.14359/8004

[15] Massey, C. "Lateral Instablity of Reinforced Concrete Beams Under Uniform Bending Moments", ACI Journal Proceedings, 64(3), pp. 164–172, 1967.
https://doi.org/10.14359/7552

[16] Sapkás, Á., Kollár, L. P. "Lateral-torsional buckling of composite beams", International Journal of Solids and Structures, 39(11), pp. 2939–2963, 2002.
https://doi.org/10.1016/S0020-7683(02)00236-6

[17] Bärnkopf, E., Jáger, B., Kövesdi, B. "Lateral-torsional buckling resistance of corrugated web girders", Pollack Periodica, 18(3), pp. 1–7, 2023.
https://doi.org/10.1556/606.2023.00797

[18] Badari, B., Papp, F. "On Design Method of Lateral-torsional Buckling of Beams: State of the Art and a New Proposal for a General Type Design Method", Periodica Polytechnica Civil Engineering, 59(2), pp. 179–192, 2015.
https://doi.org/10.3311/PPci.7837

[19] Sherbourne, A. N., Pandey, M. D. "Elastic, lateral-torsional stability of beams: Moment modification factor", Journal of Constructional Steel Research, 13(4), pp. 337–356, 1989.
https://doi.org/10.1016/0143-974X(89)90035-7

[20] Mast, R. F. "Lateral Stability of Long Prestressed Concrete Beams Part 1", PCI Journal, 34(1), pp. 34–53, 1989.
https://doi.org/10.15554/pcij.01011989.34.53

[21] Mast, R. F. "Lateral Stability of Long Prestressed Concrete Beams-Part 2", PCI Journal, 38(1), pp. 70–88, 1993.
https://doi.org/10.15554/pcij.01011993.70.88

[22] Mottram, J. T. "Lateral-torsional buckling of thin-walled composite I-beams by the finite difference method", Composites Engineering, 2(2), pp. 91–104, 1992.
https://doi.org/10.1016/0961-9526(92)90048-B

[23] Helwig, T. A., Frank, K. H., Yura, J. A. "Lateral-Torsional Buckling of Singly Symmetric I-Beams", Journal of Structural Engineering, 123(9), pp. 1172–1179, 1997.
https://doi.org/10.1061/(ASCE)0733-9445(1997)123:9(1172)

[24] Stratford, T. J., Burgoyne, C. J. "Lateral stability of long precast concrete beams", Proceedings of the Institution of Civil Engineers - Structures and Buildings, 134(2), pp. 169–180, 1999.
https://doi.org/10.1680/istbu.1999.31383

[25] Revathi, P., Menon, D. "Estimation of critical buckling moments in slender reinforced concrete beams", ACI Structural Journal, 103(2), pp. 296–303, 2006.
https://doi.org/10.14359/15188

[26] Lee, J. H., Kalkan, I. "Experimental and analytical investigation of lateral-torsional buckling of RC beams with geometric imperfections", Applied Mechanics and Materials, 479–480, pp. 1133–1138, 2014.
https://doi.org/10.4028/www.scientific.net/AMM.479-480.1133

[27] Yücesoy, A., Coşkun, S. B. "Lateral-Torsional Stability of Rectangular Prismatic Beams Using Some Analytical Approximation Techniques", International Journal of Structural Stability and Dynamics, 20(2), 2050027, 2020.
https://doi.org/10.1142/S0219455420500273

[28] Hameedi, W. S., Völgyi, I. "Experimental Investigation of Lateral Stability of a Longitudinally Assembled Girder Made of Precast Reinforced and Prestressed Concrete Parts", Periodica Polytechnica Civil Engineering, 69(2), pp. 482–489, 2025.
https://doi.org/10.3311/PPci.38183

[29] Cervenka Consulting "ATENA-GiD, (2023)", [computer program] Available at: https://www.cervenka.cz/products/atena/ [Accessed: 29 January 2025]

[30] Abed, M. A., Alkurdi, Z., Kheshfeh, A., Kovács, T., Nehme, S. "Numerical Evaluation of Bond Behavior of Ribbed Steel Bars or Seven-wire Strands Embedded in Lightweight Concrete", Periodica Polytechnica Civil Engineering, 65(2), pp. 385–396, 2021.
https://doi.org/10.3311/PPci.16689

[31] Roszevák, Z., Haris, I. "Finite Element Analyses of Cast-in-situ RC Flat Slab with an Equivalent Frame for Horizontal Loads", Periodica Polytechnica Civil Engineering, 68(1), pp. 289–304, 2024.
https://doi.org/10.3311/PPci.21896

[32] Szinvai, S., Kovács, T. "Numerical modelling of the bond behaviour between uncracked concrete and deformed steel and fibre reinforced polymer bars", In: di Prisco, M., Meda, A., Balázs, G. L. (eds.) Proceedings of the 14th fib International PhD Symposium in Civil Engineering, Rome, Italy, 2022, pp. 621–628. ISBN 978-2-940643-17-2